DTU Library

Impact of an offshore wind farm on wave conditions and shoreline development

Christensen, Erik Damgaard; Kristensen, Sten Esbjørn ; Deigaard, Rolf

Link back to DTU Orbit

IMPACT OF AN OFFSHORE WIND FARM ON WAVE CONDITIONS AND SHORELINE DEVELOPMENT

Erik Damgaard Christensen[1], Sten Esbjørn Kristensen[2] and Rolf Deigaard[2]

The influence of offshore wind farms on the wave conditions and impact on shoreline development is studied in a generic set-up of a coast and a shoreline. The objective was to estimate the impact of a typical sized offshore wind farm on a shoreline in a high wave energetic environment. Especially the shoreline's sensitivity to the distance from the OWF to the shoreline was studied. The effect of the reduced wind speed inside and on the lee side of the offshore wind farm was incorporated in a parameterized way in a spectral wind wave model. The shoreline impact was studied with a one-line model.

Keywords: Wave energy, offshore wind farm, Spectral wind wave model, Littoral transport, and shoreline development

INTRODUCTION

During recent years the relative shallow waters in the North Sea and the inner Danish waters and the Baltic Sea have been subject to an intense planning and construction of offshore renewables, mainly offshore wind farms (OWF), but lately also wave energy converters and tidal turbines. Other marine facilities that also can have a substantial impact on the wave climate, such as fish cages for aquaculture and production areas for seaweed might be installed in the future. The facilities might have local and regional impact on the wave and current conditions and therefore also on for instance sediment transport, and on the shoreline development.

Some studies have examined the influence on shoreline development due to wave energy converters, see for instance (Abanades et al., 2014; Mendoza et al., 2014; Millar et al., 2007). The effect from offshore wind farms on shoreline have gained minor attention compared to the wave energy converters (WEC), even though that the number of installed offshore wind farms is much higher than the few installations of WEC-farms. A few studies have addressed the impact on the wave field, see for instance (Christensen et al., 2013; McCombs et al., 2014; Ponce de León et al., 2011). The research presented in this paper concentrates on the effect of a typical offshore wind farm on the shoreline development.

(Christensen et al., 2013) describes the impact of offshore wind farms on the wave conditions. Generation of wind waves is governed by the surface shear stress on the water surface due to the wind, the fetch, the depth and the duration of the storm. When the waves meet the offshore wind farm the wave field can be altered due to three significant processes that have to be considered, which are; A) the dissipation due to drag resistance, B) reflection/diffraction of waves around the structure, and C) the effect of a changed wind field inside and on the lee side of the offshore wind farm. The turbines in operation extract energy from the wind but also act as obstacles to the wind. These two processes change the wind field inside and on the lee side of the wind farm. These effects were studied by implementing parameterised models in the spectral wind wave model MIKE21 SW. The implementation will be summarised in this paper.

The size of offshore farm was inspired by two of the first larger scale offshore wind farms in Danish waters and in the world; Horns Reef Offshore Wind Farm I and Nysted Offshore Wind Farm. Aerial photographs of the OWF's can be seen in (Christiansen and Hasager, 2005), which indicate that the size of the OWF is in the order of 5 km x 5 km. If the OWF has another size, for instance larger, the results might not be transferred or scalable.

In this paper a parametric study in carried out in order to examine the impact on a straight and stable shoreline. The shoreline development is modelled with LittoralProcessesFM, in which the one-line model can be used to analyse shoreline development over relative long time-span; typically decades. Based on characteristic wind conditions in the North Sea a synthetic wave climate was elaborated with MIKE21 SW that included the effect of the OWF.

The structure of the paper is as follows. The methodology on how the modified wind field and foundations were parameterised is given in the following chapter. This is followed by a description of the data used for the study and an introduction to the shoreline development tool LITLINE. The fourth chapter describes the synthetic study that was carried out. This is followed by chapters on discussions and conclusions.

[1] Technical University of Denmark, DTU-MEK, Nils Koppels Alle' Build 403, DK-2800, Kgs. Lyngby, Denmark
[2] DHI, Agern Alle' 5,DK-2970 Hørsholm, Denmark

PARAMETATION OF THE EFFECTS OF THE OWF ON WAVE CONDITIONS

Three major effects were considered in (Christensen et al., 2013) which were A) the drag dissipation due to for instance separation of the flow around the foundation, B) the diffraction /reflection of wave energy, and C) the reduced water surface friction inside and on the lee side of the OWF. It was realised that the drag dissipation of energy was much smaller compared to the other two effects, and therefore this will be neglected in the following analyses.

The effect of the diffraction/reflection of wave energy flux

The effect of the diffraction and reflection was studied by examining the transmitted wave energy behind a foundation supporting an offshore wind turbine. The diffraction problem is traditionally divided into the incoming and scattered velocity potential. The sum of the two constitutes the diffraction potential. By limiting the study to 1st order stokes waves the transmitted wave energy can be found by the following integration:

$$\hat{E}_{f,transmitted} = \int_{CL}^{\infty}\left[\frac{1}{T}\int_0^T\int_{-h}^0 (p_{in}^+ + p_{scat}^+)(u_{in} + u_{scat})dzdt\right]ds \tag{1}$$

$\hat{E}_{f,transmitted}$ is the integrated wave energy flux from a centre-line at the structure to infinity. p_{in}^+ and p_{scat}^+ is the excess pressure for the incoming and scattered wave, and u_{in} and u_{scat} is the incoming and scattered horizontal particle velocity. T is the wave period and h is the water depth. In order to establish the velocity potentials for a generally shaped foundation the panel method WAMIT^{TM}, (Newman et al., 1995) was used. Additionally an asymptotic solution was added as the integral is a sum of a numerical part in the vicinity of the structure and an analytical part for the integration going to infinity. In this way the transmitted wave energy flux was found and compared to the incoming wave energy flux. In this study the supporting structure from the water surface to the sea-bed was assumed to be a monopile. The difference, which will be the reflected wave energy flux, was then normalised by the total incoming wave energy over a width equal to the diameter of the cylinder.
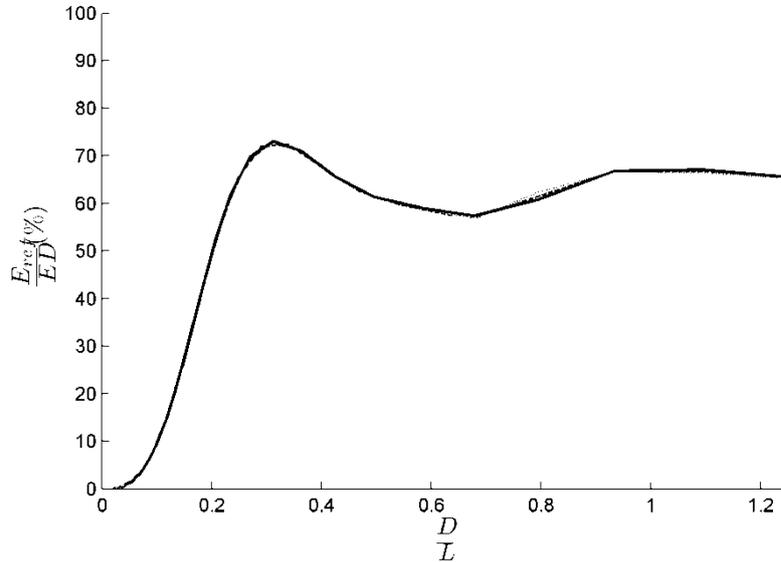
Figure 1   **The percentage of reflected wave energy flux** $\dfrac{E_{reflec}}{E \cdot D}$ **as function of the diameter, D, over the wave length, *D/L***

As $D/L \rightarrow \infty$ the waves will act as a wave ray, and therefore the wave and energy will be reflected at the surface of the structure and therefore ingoing and outgoing angles will be the same. Therefore the reflected wave energy will go towards 70.7 % as $D/L \rightarrow \infty$, which the curve in Figure 1 clearly supports.

For a circular cylinder the amount of reflected wave energy is a simple function of the ratio between the diameter and the wave length; D/L.

The reduced wind surface shear inside and on the lee side of the offshore wind farm

The effect of an offshore wind farm on the shear stress at the ocean surface has been estimated by the use of a SAR (Synthetic Aperture Radar). Data from both satellite and air craft mounted instrumentation have been used, analyses and reported in (Christiansen and Hasager, 2005; Christiansen et al., 2006).

The geophysical model functions used for SAR wind retrieval at the standard height 10 m apply to open oceans and neutral atmospheric stability. For such conditions we can determine the corresponding friction velocity, u_*, from the logarithmic wind profile with reasonable assumptions about the roughness. This friction velocity becomes roughly proportional to the model function wind speed U_{10}. Since u_* is intimately connected and adapt very fast to the wave spectrum at the radar wave lengths, it was concluded in (Christensen et al., 2013) that we can obtain the change of u_* from the radar measurements, as being roughly proportional to the change of U_{10}, even in the perturbed flow within and just behind the wind farm.

From the measurements the reduction of the wind velocity in and behind an offshore wind farm can be taken into account by introducing a correction of the friction velocity

$$u_* = f_w u_*^0 \tag{2}$$

where f_w is the correction factor and u_*^0 is the undisturbed wind friction velocity. Based on the field measurements cited above a simple formulation for the correction factor is given by

$$f_w = 1 - 0.1 \left(\frac{x}{L} \right)^{3/2} \qquad 0 \le x \le L \tag{3}$$

$$f_w = 1 - 0.1 e^{-\frac{(x-L)}{L}} \qquad x > L \tag{4}$$

Here u_*^0 is the undisturbed wind friction velocity, x is the distance in the same direction as wind from the start of the wind farm, and L is the length of the wind farm. The correction factor for the friction velocity is applied before the calculation of the sea roughness. The approach assumes that the effect of the reduced surface shear is evenly distributed around and between the offshore wind turbines. This means that the offshore wind farm is regarded as a continuum. The spatial extension of the correction factors will depend on the wind direction, which must be accounted for when using the equations (3) and (4).When an offshore wind farm is based on larger wind turbines the spacing between them increases as well. Therefore the model might not have to be changed for other configurations as the fraction of extracted energy from the wind is the same. However for much larger areas covered with offshore wind turbines or very different configurations the model might have to be modified.

The implementation in a spectral wind wave model

For modelling of the wave conditions the MIKE 21 SW Spectral Wave Model was used. Using the fully spectral formulation in MIKE 21 SW Spectral Wave Model, the dynamics of the gravity waves are described by the transport equation for wave action density. This section gives an introduction to the method and describes the steps necessary to include the effect from structures and from wind speed reduction.

The wave action density spectrum varies in time and space and is a function of the relative angular frequency,$\sigma = 2\pi f$, and the wave direction, θ. The action density,$N(\sigma, \theta)$, is related to the energy density $E(\sigma, \theta)$ by:

$$N = \frac{E}{\sigma} \tag{5}$$

The governing equation is the wave action balance equation formulated in either Cartesian or spherical co-ordinates, see (Komen et al., 1994), and (Young, 1999). In horizontal Cartesian co-ordinates, the conservation equation for wave action can be written as:

$$\frac{\partial N}{\partial t} + \nabla \cdot \left(\overline{vN} \right) = \frac{S}{\sigma}$$

(6)

where $N(\vec{x}, \sigma, \theta, t)$ is the action density, t is the time, $\vec{x} = (x, y)$ is the Cartesian co-ordinates, $\vec{v} = (c_x, c_y, c_\sigma, c_\theta)$ is the propagation velocity of a wave group in the four-dimensional phase space $\vec{x}, \sigma$ and θ, and S is the source term for the energy balance equation. ∇ is the four-dimensional differential operator in the $\vec{x}, \sigma, \theta$ -space. The source term S is described as a sum of several source and sink terms:

$$S = S_{in} + S_{nl} + S_{we} + S_{bf} + S_{wb}$$

(7)

More details on the numerical algorithms and discretisation can be found in (Christensen et al., 2013; Sørensen et al., 2004).

The effect of diffraction/reflection around the structure

The effect of the reflection/diffraction of wave energy by the wind turbine foundations was included by the changed direction of the wave energy directly in the convective terms. The contribution to the time-derivative of the cell-centered value of the wave action density is managed by the $N_{i,l,m} = N(\vec{x}_i, \sigma_l, \theta_m)$, from the convective transport in the geographical space into the cell i. The implementation in MIKE21 SW is described in detail in (Christensen et al., 2013). A crucial part is the reflection factor, c, which was obtained as described in the previous chapter 2. For simplicity it was assumed that the energy was reflected 180 degrees.

The effect of the modified surface shear stress due to the offshore wind farm

The reduced water surface shear stress modifies the source term S_{in} in eqs. (7). The background for wind generation of waves can be found in for instance (Janssen, 1991, 1989) . In MIKE21 SW the input source term, S_{in} is formulated as:

$$S_{in}(f, \theta) = \max(\alpha, \gamma E(f, \theta))$$

(8)

where α is the linear growth, γ is the nonlinear growth rate and $E(f, \theta)$ is the energy density. For a given wind speed and direction, the nonlinear growth rate of a given frequency and direction depends on the friction velocity, u_* and sea roughness, z_0.

The linear growth rate, α, is included to trigger the growth of ocean waves. In many operational waves models this mechanism is ignored as real ocean waves will be present to trigger the wave growth. In the spectral wave model used in this study, MIKE21 SW, the linear growth rate was only used until the non-linear model is larger. Both the linear and non-linear growth rate depend on the surface friction velocity, u_*, and the sea roughness, z_0. The way to find these is described in detail in (Christensen et al., 2013) along with the linear and non-linear growth models. The reduction of the wind velocity in and on the lee side of an offshore wind farm was taken into account by introducing a correction of the friction velocity as specified in eqs. (2), (3) and (4).

MODEL SET-UP AND DATA FOR THE ANALYSES

The test-case to analyse the effect of the offshore wind farm was based on a synthetic case. The fetch normal to a long and uniform coastline was set to 200 km. The coastline was situated at the east and the limiting land to the west. The ocean was infinite to the northern and southern directions, wherefore the actual fetch length was longer than 200 km for wind directions larger and smaller than 270 °. The water depth was set equal to 20 m.

The model set-up was based on a full spectral model with 25 frequencies with a minimum frequency of 0.04 Hz increasing with 11.5 % for each increment. In the directional discretization 36 directions were used for all 360°. The sea surface roughness was found from the uncoupled model with the Charnock parameter equal to 0.0185, which was based on the findings in (Wu, 1980). Source terms for white capping (deep-water wave breaking) and quadruplet-wave interaction were included in modelling the waves. Bottom roughness was included in the simulation based on the formulation outlined in (Johnson and Kofoed-Hansen, 2000). The equivalent Nikuradse sand roughness was set to 1 cm.

The model was set-up using an unstructured grid to resolve the computational domain. The domain and grid is illustrated in fig 2. The grid consisted of three regions. In the inner region the cells

were quadratic with a side length of 250 m. In the intermediate region triangular cells had a typical side length of 500 m. The last and coarsest grid, the outer region, also consists of triangular cells, but with a typical side length of 1000 m.
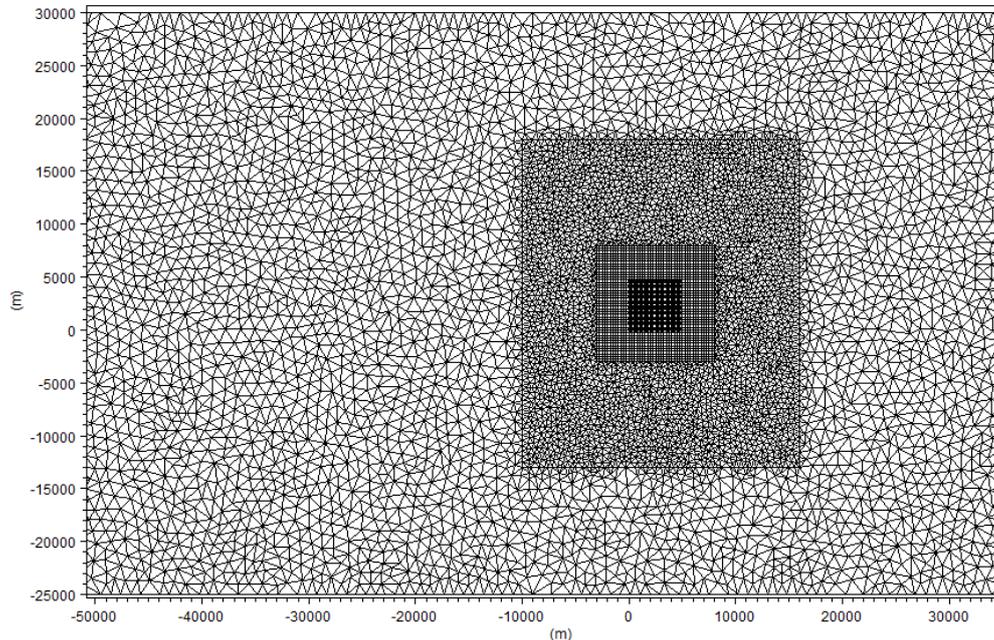
Figure 2   A close up of the unstructured grid used in the spectral wind wave modelling.

In (Christensen et al., 2013) the implementation of different wind direction in the modelling was not addressed. Different alternatives for including the reduced wind speed inside and on the lee side were investigated. A simplification of the method where the surface shear stress was reduced with 10% inside the area of the OWF was tested. It turned out that this did not reproduce the wind field in the same way as the method outline in the previous section as indicated in Figure 3. The figure shows the fraction between significant wave height with, and without an OWF, $H_{m0}/H_{m0,noOWF}$, along the centerline of the OWF in the wind direction. The OWF was situated for a distance (Dist), between 0 and 5 km. For shorter fetches the maximum reduction of the significant wave height was for this case around 4 %, as shown by the full line with squares. For a fetch length of 200 km the reduction is around 1-2 % for a wind speed of 20 m/s. The results for the simplified approach are shown with the punctured line with plusses. The simplified approach reduced the effect of the OWF up to around 50% 10 km down-wind of the wind farm. Therefore the simplified approach was not applied.

As seen from the initial investigations it was necessary to rotate the field of the reduction factor for the surface shear stress velocity. This might seem to be a simple task, however the length L in the formulation of the correction factor f_w in eqs. (3) and (4) is not constant in the wind direction when it is not aligned with the sides in the OWF. Due to the relative simplicity of the model for the correction factor field the field was first found for an orientation of 270°, i.e. the wind goes from west to east. Then this field was rotated for instance 35° around the centerline of the lee side of the OWF for a wind direction from 305° (Wind coming from approximately NorthWest). Figure 4 shows an example of the procedure as outlined above. The rotated correction factor field was used for all cases with wind coming from 305°, while the wind speed might vary. One could argue that the rotation of the correction factor field should have been made around the center of the OWF. However the scarceness of the data and the small angles of rotation used in this study suggests that the used procedure was acceptable.

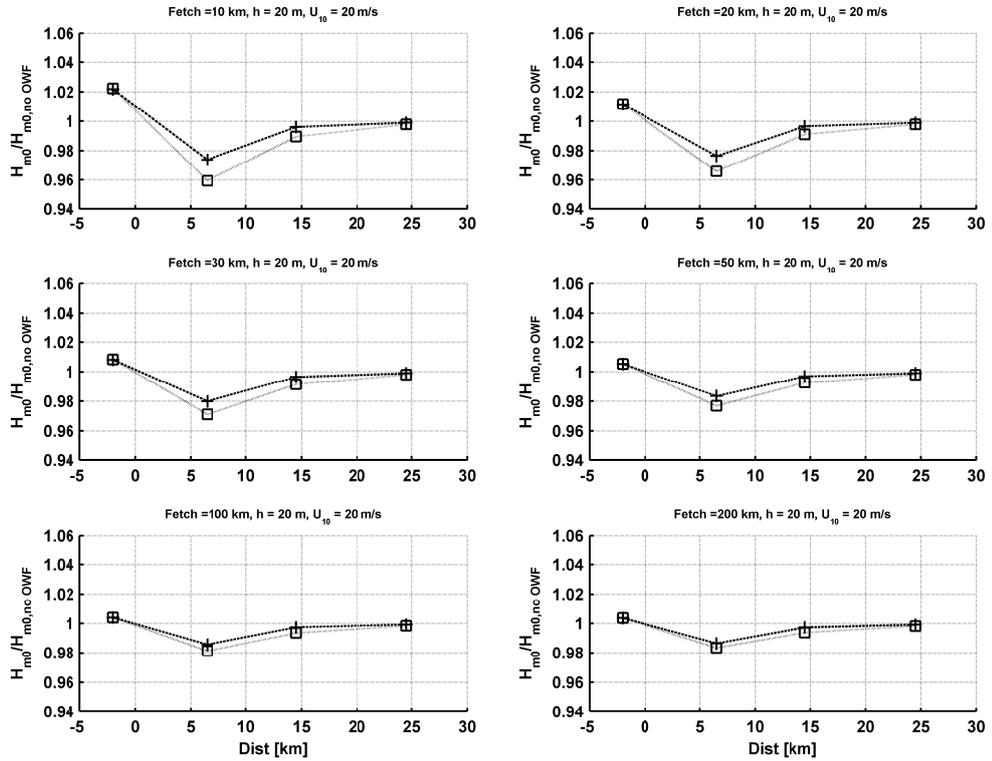**Figure 3**   The full lines with □ show the original formulation, and the punctured lines with + the attempt to use a modified reduction factor of the surface shear stress.
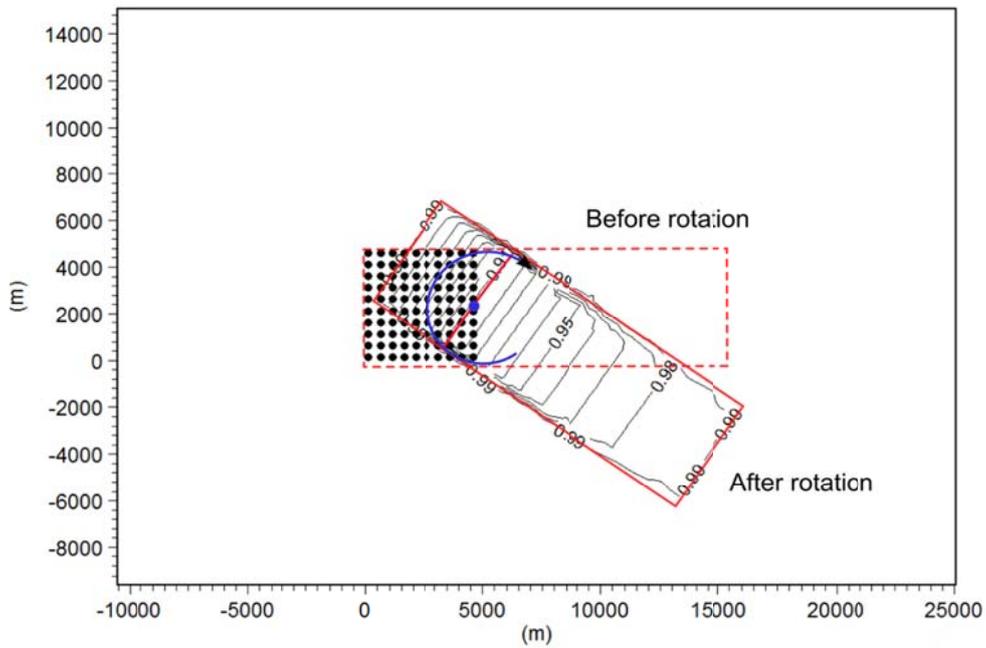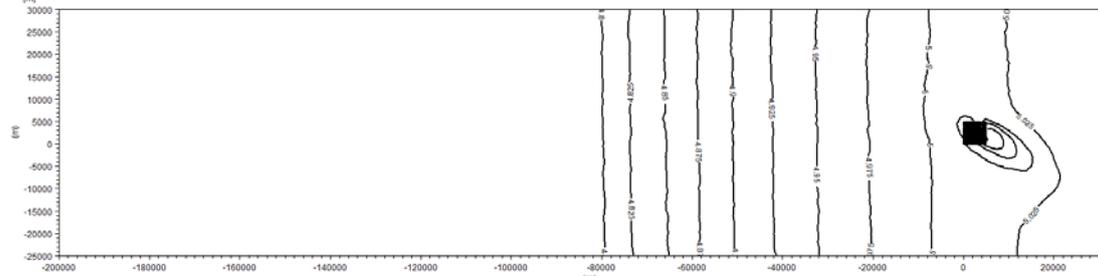

Figure 4   Rotation of the correction factor field f_w, when the wind direction was changed from 270° to 305°.

In Figure 5 and Figure 6 an example of the significant wave height distribution, H_{m0}, is shown. The wind speed was 24 m/s, and the direction of the wind 305°. This event had an occurrence of 0.003% as shown in Table 1. In the close-up in Figure 6 the structures reflected a part of the wave energy leading to an increase in in the Northwestern corner of the OWF. Inside and on the lee side the presence of the OWF reduced the wave height compared to outside of the affected area.
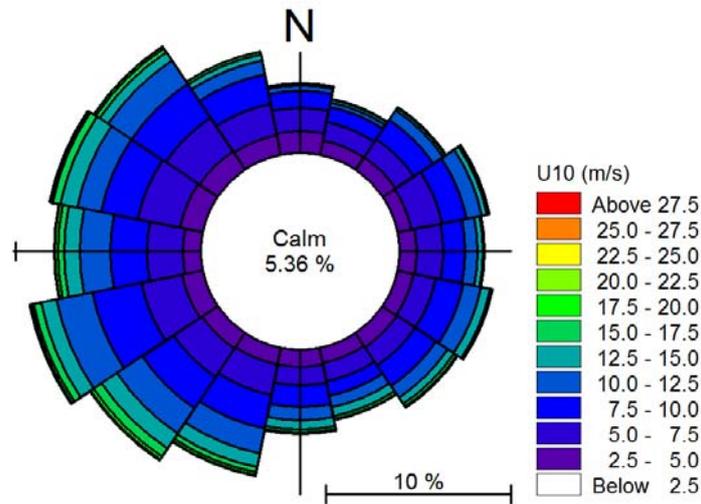

Figure 5　An example of the wave height distribution around the OWF, for a wind direction of 305°, and a wind speed of U_{10} = 24 m/s.

Figure 6　Close-up of example shown in Figure 5 of the wave height distribution around the OWF, for a wind direction of 305°, and a wind speed of U10 = 24 m/s.

Wind data

To have a realistic idea of the wind field in the North Sea, and other neighbouring areas a time series of the wind speed and direction was extracted in the North Sea from NCEP's CFSR model. The data was extracted at longitude 7.5 and latitude 56.1. The data covers a period from the 15th December 2007 to 31st of December 2011, with one hour intervals. A wind rose in Figure 7 shows the wind speed and directions. As expected this climate zone the wind speed is dominated by westerly winds, but land might also play a role on the magnitude of the wind speed.

Based on the extracted wind time series a scatter diagram was elaborated and shown in Table 1. Here wind directions outside the westerly interval from 230° to 310° was left out as these directions only have small impact on a coastline east of the OWF. Wind speeds less than 6 m/s were left out as well. With the intervals indicated in the table this gave 37 wind conditions to be analysed in MIKE21 SW, where the data was set to the middle of the interval. This means that the first in the upper left corner in the table had a wind direction of 235°, and a wind speed of 8.0 m/s.

**Figure 7   Wind rose for the extracted wind data**

Table 1   Scatter diagram of the wind data used in the analyses. The data originates from NCEP's CFSR model. Wind speeds in m/s, wind directions are relative to True North.

Dir/U10	6-10	10-14	14-18	18-22	22-26
230-240	1.66%	1.17%	0.34%	0.07%	0.01%
240-250	1.97%	1.21%	0.34%	0.06%	0.03%
250-260	1.78%	1.04%	0.28%	0.09%	0.01%
260-270	1.56%	1.19%	0.26%	0.08%	0.01%
270-280	1.26%	0.85%	0.26%	0.06%	---
280-290	1.40%	0.76%	0.41%	0.04%	---
290-300	1.55%	0.85%	0.34%	0.07%	---
300-310	1.67%	0.90%	0.28%	0.06%	0.003%

ESTIMATION OF SHORELINE DEVELOPMENT ON AN LONG AND STRAIGHT COAST
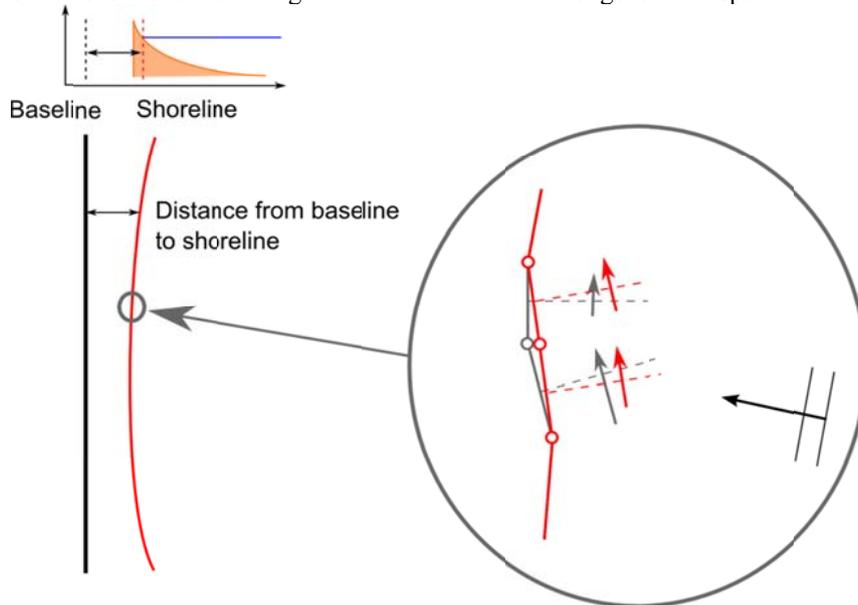
The shoreline model

LittoralProcessesFM is a deterministic numerical modelling system which describes the major processes in the nearshore zone. The modelling system is based on one-dimensional modules for wave transformation across a specific coastal profile (which can include bar trough features); a hydrodynamic module which calculates wave driven currents and water level variations; and DHIs sand transport model STP which calculates non-cohesive sand transport in a wave-current flow regime.
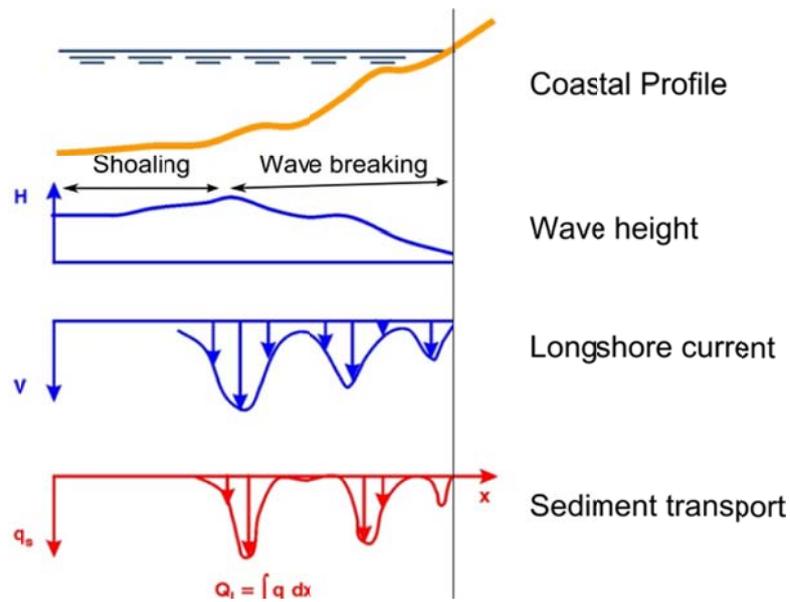
Figure 8   Calculation of longshore transport in LittoralProcesses FM includes: Transformation across a specific coastal profile, Calculation of wave driven currents and finally calculation of longshore transport due to combination of waves and currents.

Shoreline evolution is implemented using a standard shoreline model which moves shoreline nodal points onshore/offshore based on the gradient in the calculated longshore transport.

Figure 9   Shoreline evolution is implemented as a standard shoreline model where nodal points are moved onshore/offshore according to gradients in the littoral transport.

Model setup
Primary parameters for the model set-up was based on relatively fine sediment where the median grain diameter was, $d_{50} = 0.14$ mm, and with a geometrical spreading of $\sigma_{geo} = 1.5$. The active height of coastal profile was, $H_{act} = 7.0$ m. The coastline update frequency was 1 year.

Q-alpha curve for real climate
The littoral drift for the wave climate derived from a point along the West Coast of Denmark has been calculated for a shore normal of 262 deg. N and for variations within ±15 deg. This leads to a so-called Q-alpha relationship which illustrates the sensitivity of the littoral transport to changes in

shoreline orientation. The Q-alpha relationship is shown in Figure 10. For a shore normal of 262 deg.N (indicated with a black vertical line) there was a net transport towards south of 116,000 m^3/yr and a gross transport of 1,200,000 m^3/yr. An anti-clockwise rotation of the shore normal will increase the southward component of the longshore transport and vice versa. According to the figure relatively small changes in the direction of the shore normal (or the predominant wave direction) can have significant changes on the net annual transport. As an example, the net transport is doubled for a 3 deg. change in orientation (anti-clockwise) of the shore normal.
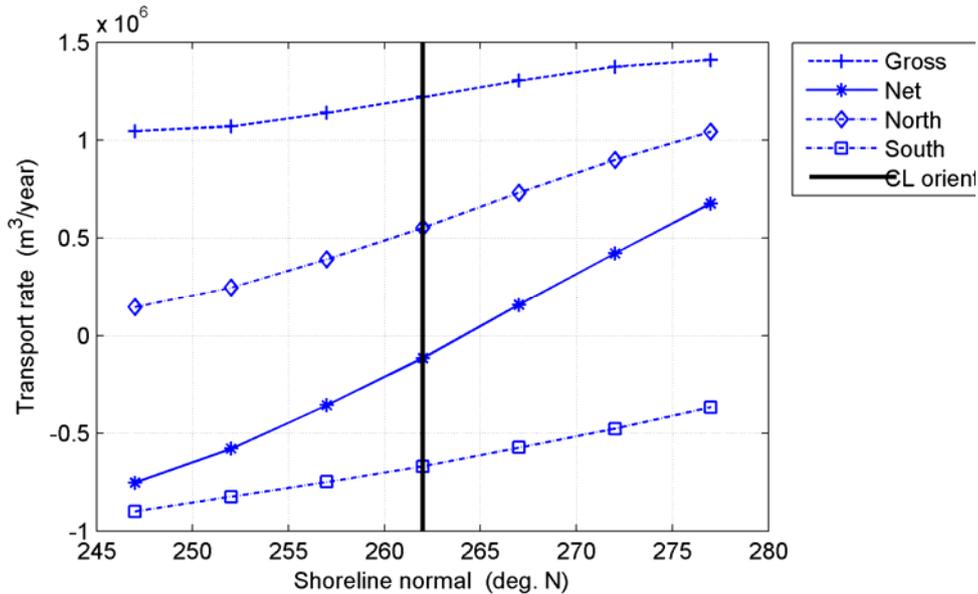

Figure 10   Sensitivity of longshore transport to different shoreline orientations. The initial shoreline orientation used in the shoreline evolution simulations is indicated in black.

Shoreline impact

The lee effects of the OWF results in sediment accumulations similar to what can be seen behind shore parallel offshore breakwaters. The sediment accumulation is in the form of a salient. The volume of sand required to build the salient is taken from the neighbouring beaches thus leading to shoreline erosion.

Figure 11 shows predicted shoreline changes for three different cases covering a period of 100 years. The OWF was in all three cases located between alongshore distances 20km and 25km. In the top panel, the OWF was located 5 km from the coast (measured from the landward tip of the OWF). This case leads to the largest shoreline changes, where the shoreline advances approximately 50 m seaward. The maximum protrusion of the salient was lower for the cases where the OWF is located further from the coast. The alongshore footprint of the effect of the OWF increases however with the distance between the OWF and the coastline. The above described sensitivity of salient shape to the distance between the OWF and the coastline agrees with accepted behaviour of salients located in the lee of shore parallel offshore breakwaters; see e.g. (Kristensen et al., 2013).
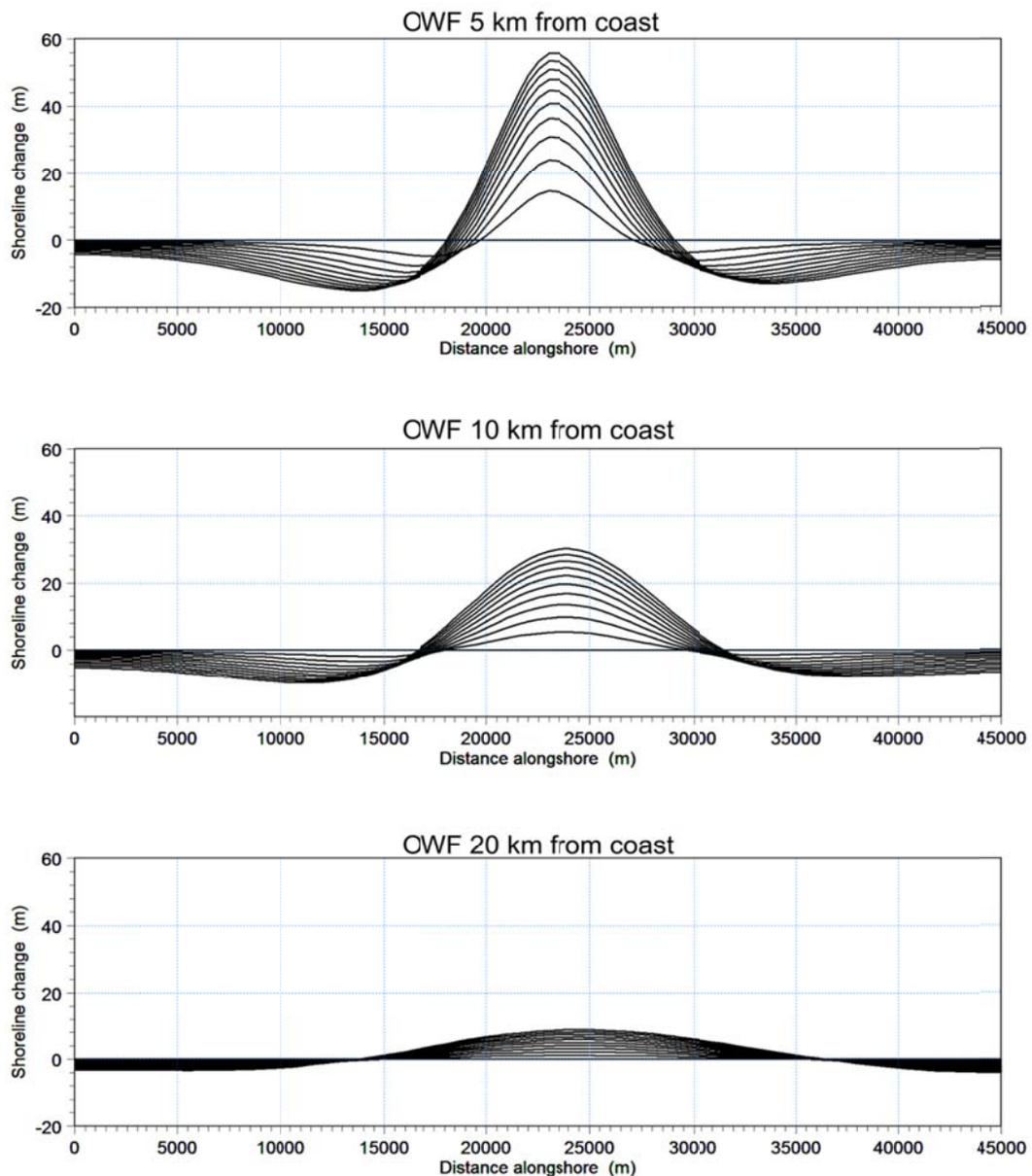
Figure 11 Sensitivity of the shoreline impact for different locations of the Offshore wind farm. The shoreline envelopes are shown at intervals of 10 years (each panel shows 100 years shoreline evolution).

DISCUSSION

The use of the correction factor for the surface friction velocity has not been compared directly to field measurements of wave fields around an OWF. The reduction of the wave height is in general moderate, and therefore it might not be an easy task to collect very high qualitative data from the field. Many aspects have to be considered when setting up field campaign to examine the impact directly in the field. Firstly, data on the wind field should be known in detail. Further the location of the wind farm and limiting land regions is another important aspect. The wave field has to be measured in several points, at last 5- 10 points along the wind direction. Finally the coastal development of the coastal stretches that might be influenced by the OWF, up to around 30 km from the OWF, should be measured. These data must be collected simultaneously for a longer time-span. The intervals of the coastline measurements can of course be much larger than for the other data. This could turn out to be a substantial field campaign, and therefore the question arises whether the presented analyses over predicts the impact. Would it be worth and is it necessary to address the impact in for instance coastline development studies? This is of course difficult to answer without firm data, but there are a couple of issues that should be noted. First of all the fetch is moderate, around 200 km. In many places

in the North Sea the fetch could easily be 500 km or more. This will increase the wave height in general around the OWF and also along the coastal stretches in the lee side of the OWF. Secondly the wave analyses were based on un-coupled growth models. Using a coupled model as presented in, (Janssen, 1991), might modify the impact. Preliminary analyses showed that the use of the coupled model enhanced the effect of the OWF inside and on the lee side of the OWF. As it was not possible to make a direct comparison with field measurements a comparison was made to a parametric growth model in (Christensen et al., 2013), where a good agreement between the simple fetch model and the uncoupled growth model in MIKE21 SW was achieved. However the model should be compared to field data to improve credibility. Here the use on the decoupled model could show to be un-conservative, meaning that the actual impact on the wave field was larger in nature, than the impact found based on the un-coupled model.

The predicted shoreline impact to OWF's indicates that the impact of an OWF on the shoreline can lead to large areas with sediment accumulation as well as neighbouring areas with a sediment deficit. For the considered climate (typical North Sea climate) and the spatial scales considered, the morphological time scales involved are medium to long term, i.e. morphological evolution will continue to occur several decades.

The study therefore suggests that a shoreline impact should be considered as part of any EIA of new OWF. This may initially be considered as part of a screening such as the present study where the effect of the OWF is first simulated by use of a few sea-states which can be used to describe the annual wave climate and then combine this with a shoreline model for the shoreline impact predictions. In case the screening suggests significant changes, a more detailed study should be developed.

CONCLUSIONS

Based on wind data from the North Sea a synthetic study on the impact of an OWF on wave conditions and shoreline developments was carried out. The study combined parametric models for the following effects:
- Diffraction and reflection from the support structures for the offshore wind turbines
- Reduced wind speed inside and on the lee side of the Offshore Wind Farm (OWF)

The effects were in parameterised form implemented in the spectral wind wave model, MIKE21 SW. The shifting orientation of the wind field had to be incorporated by turning the field of the correction factor along with the wind direction.

37 wind events were established and the field was found for a fetch of around 200 km. The fetches were larger for north-westerly and south-westerly wind directions. Based on the modelled wave conditions the shoreline evolution was analysed for three distances from the lee side on the OWF, 5 km, 10 km and 20 km. Moderate impact was found for the largest distance, while the other two distances showed a significant progression of the shoreline after 100 years of 50 m and 30 m, respectively.

The impact was considered to be non-conservative. Firstly, the impact of the OWF on the wave conditions was sensitive to the choice of growth model. The un-coupled growth model seemed to be less sensitive to the OWF compared to the coupled model. Secondly, the lack of good quality data increases the uncertainty of the analyses.

It was suggested that the effect of an offshore wind farm on adjacent shores should be a part of environmental impact assessments for new OWF's.

ACKNOWLEDGMENTS

REFERENCES

Abanades, J., Greaves, D., Iglesias, G., 2014. Coastal defence through wave farms. Coast. Eng. 91, 299–307.

Christensen, E.D., Johnson, M., Sørensen, O.R., Hasager, C.B., Badger, M., Larsen, S.E., 2013. Transmission of wave energy through an offshore wind turbine farm. Coast. Eng. 82, 25–46.

Christiansen, M., Hasager, C., 2005. Wake effects of large offshore wind farms identified from satellite SAR. Remote Sens. Environ. 98, 251–268.

Christiansen, M.B., Hasager, C.B., Labora-, R.N., 2006. for Wake Mapping Offshore. Offshore (Conroe, TX) 437–455.

Janssen, P.A.E.M., 1989. Wave-Induced Stress and the Drag of Air Flow over Sea Waves. J. Phys. Oceanogr. 19, 745–754.

Janssen, P.A.E.M., 1991. Quasi-linear theory of wind wave generation applied to wave forecasting. J. Phys. Ocean. 21, 1631–1642.

Johnson, H., Kofoed-Hansen, H., 2000. Influence of Bottom Friction on Sea Surface Roughness and Its Impact on Shallow Water Wind Wave Modeling. J. Phys. Ocean. 30, 1743–1756.

Komen, G.J., Cavaleri, L., Doneland, M., Hasselmann, K., Hasselmann, S., Janssen, P.A.E.M., 1994. Dynamics and modelling of ocean waves. Cambridge University Press, UK.

Kristensen, S.E., Drønen, N., Deigaard, R., Fredsoe, J., 2013. Hybrid morphological modelling of shoreline response to a detached breakwater. Coast. Eng. 71, 13–27.

McCombs, M.P., Mulligan, R.P., Boegman, L., 2014. Offshore wind farm impacts on surface waves and circulation in Eastern Lake Ontario. Coast. Eng. 93, 32–39.

Mendoza, E., Silva, R., Zanuttigh, B., Angelelli, E., Lykke Andersen, T., Martinelli, L., Nørgaard, J.Q.H., Ruol, P., 2014. Beach response to wave energy converter farms acting as coastal defence. Coast. Eng. 87, 97–111.

Millar, D.L., Smith, H.C.M., Reeve, D.E., 2007. Modelling analysis of the sensitivity of shoreline change to a wave farm. Ocean Eng. 34, 884–901.

Newman, J.N., Lee, C.H., Korsmeyer, F.T., 1995. WAMIT version 5.3. A radiation Diffraction panel Program for Wave-body Interactions.

Ponce de León, S., Bettencourt, J.H., Kjerstad, N., 2011. Simulation of irregular waves in an offshore wind farm with a spectral wave model. Cont. Shelf Res. 31, 1541–1557.

Sørensen, O.R., Kofoed-Hansen, H., Rugbjerg, M., Sørensen, L.S., 2004. A third-generation spectral wave model using an unstructured finite volume technique, in: Smith, J.M. (Ed.), Proc. of the 29th International Conference on Coastal Engineering (ICCE). World Scientific Publishing Co. Pte. Ltd., Lisbon-Portugal, pp. 894–906.

Wu, J., 1980. Wind-Stress coefficients over Sea surface near Neutral Conditions—A Revisit. J. Phys. Oceanogr. 10, 727–740.

Young, I.R., 1999. Wind-generated ocean waves. In Elsevier Ocean Engineering Book Series, Vol. 2. Eds. R. Bhattacharyya and M.E. McCormick, Elsevier.